Quantity of Intraretinal Hyperreflective Foci in Patients With Intermediate Age-Related Macular Degeneration Correlates With 1-Year Progression

Marco Nassisi,[1,2] Wenying Fan,[1–3] Yue Shi,[1,2] Jianqin Lei,[1,2,4] Enrico Borrelli,[1,2,5] Michael Ip,[1,2] and Srinivas R. Sadda[1,2]

[1]Doheny Image Reading Center, Doheny Eye Institute, Los Angeles, California, United States
[2]Department of Ophthalmology, David Geffen School of Medicine at UCLA, Los Angeles, California, United States
[3]Beijing Tongren Eye Center, Beijing Tongren Hospital, Beijing Ophthalmology and Visual Sciences Key Laboratory, Capital Medical University, Beijing, China
[4]Department of Ophthalmology, First Affiliated Hospital of Xi'an Jiaotong University, Xi'an, China
[5]Ophthalmology Clinic, Department of Medicine and Science of Ageing, University G. D'Annunzio Chieti-Pescara, Chieti, Italy

Correspondence: Srinivas R. Sadda, Doheny Image Reading Center, Doheny Eye Institute, 1355 San Pablo Street, Suite 211, Los Angeles, CA 90033, USA; SSadda@doheny.org.

Submitted: February 18, 2018
Accepted: June 10, 2018

Citation: Nassisi M, Fan W, Shi Y, et al. Quantity of intraretinal hyperreflective foci in patients with intermediate age-related macular degeneration correlates with 1-year progression. *Invest Ophthalmol Vis Sci*. 2018;59:3431–3439. https://doi.org/10.1167/iovs.18-24143

Purpose. The purpose of this study was to evaluate the correlation between quantity of intraretinal hyperreflective foci (HRF) in the eye with intermediate AMD and progression to late AMD.

Methods. Volume optical coherence tomography (OCT) scans from 114 eyes of 114 patients were retrospectively reviewed. HRF were assessed both qualitatively and quantitatively. Five sequential en face slabs from midretina were thresholded to isolate the HRF. These five slabs were recombined, and HRF area was measured in the whole 6 × 6-mm image (HRF_{TOT}) and within the central 3-mm (HRF_{3mm}) and 5-mm (HRF_{5mm}) regions. These measurements were correlated with the development of late AMD (defined as choroidal neovascularization [CNV] and/or complete RPE and photoreceptor atrophy [cRORA]) after 1 year of follow-up.

Results. HRF area in all three regions showed significant correlations with progression to late AMD: $R = 0.610$ for HRF_{3mm}, $R = 0.622$ for HRF_{5mm}, and $R = 0.614$ for HRF_{TOT} (all $P < 0.001$). Correlations remained significant with progression to cRORA alone, though not for progression to CNV alone. While qualitative assessment of HRF (i.e., presence of HRF: yes or no) also showed a significant correlation with progression to late AMD ($R = 0.454$, $P < 0.001$) and atrophy alone ($R = 0.445$, $P < 0.001$), they were weaker than by HRF quantification.

Conclusions. The area of HRF from en face OCT in eyes with intermediate AMD correlates with the 1-year risk of progression to late AMD, and in particular with the development of atrophy.

Keywords: age-related macular degeneration, optical coherence tomography, intraretinal hyperreflective foci, age-related macular degeneration progression

AMD is the leading cause of central vision loss among elderly individuals in the developed countries.[1] AMD is a progressive neuroretinal disease in which the probability of progression from intermediate stages to advanced AMD (i.e., geographic atrophy [GA] and choroidal neovascularization [CNV]) at 5 years can be as high as 27%, rising to 43% when subjects have advanced AMD in the fellow eye.[2]

Although effective treatments are now available for CNV, there is no effective therapy for GA, with several agents having failed trials or still under assessment for preventing progression of GA.[3] Rather than attempting to intervene after atrophy has already developed, it may be preferable to prevent the development of late AMD. As such, identification of all factors that may impact the development of advanced AMD is of critical importance.

Over the past 20 years, optical coherence tomography (OCT) has become an indispensable tool for the evaluation of patients with AMD owing to its ease of acquisition and high axial resolution providing excellent visualization of retinal morphology. Recently Lei et al.[4] proposed a simple OCT-based scoring system for progression of AMD, and one of the features considered as an important risk factor for late AMD was the presence of intraretinal hyperreflective foci (HRF).

HRF are defined as discrete, well-circumscribed lesions with equivalent or higher reflectivity than the RPE band on OCT and typically associated with hyperpigmentation on color fundus photograph.[5] It has been demonstrated that there is a highly specific spatial correlation of HRF with the apex of drusen[6] and/or subretinal drusenoid deposits (SDD)[4] and that HRF overlying drusen are associated with an increased risk of atrophy at that location.[7]

The AREDS2 Ancillary SD-OCT Study reported that GA lesions detected at 2 years were significantly correlated with the presence of HRF and with a greater number of HRF at baseline.[8] To our knowledge, however, there have been no previous assessments that have precisely quantified these HRF in the macula. In this study, we retrospectively reviewed en face OCT images of intermediate AMD eyes and utilized a

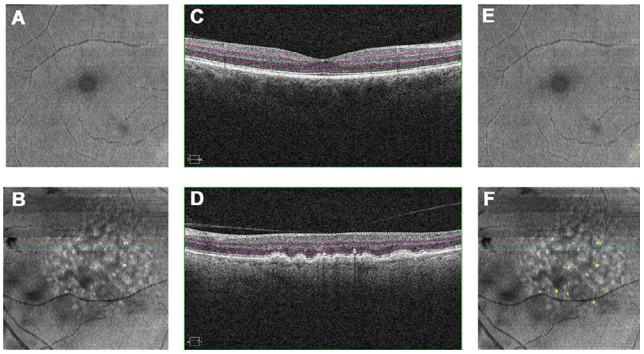

FIGURE 1. En face midretina slabs of a normal subject (**A**) and an intermediate AMD patient (**B**). The corresponding B-scans (**C**, **D**), respectively, reveal the presence of HRF in the AMD patient corresponding to the hyperreflective spots in the en face scan. The application of our thresholding method reveals almost no pixels selected in the control image (*yellow pixels*) (**E**) but a good selection of the HRF in the AMD patient (*yellow pixels*) (**F**).

semiautomated method to quantify HRF in the macular area. We correlated HRF quantity with drusen volume (DV) and ellipsoid zone (EZ) normalized reflectivity, which are well-established markers of AMD progression[9,10] and photoreceptor damage,[11–13] respectively. We then evaluated the correlation between HRF quantity and progression to advanced AMD after 1 year.

METHODS

In this retrospective study, we collected and analyzed spectral domain (SD)-OCT images of consecutive patients with intermediate AMD[14] acquired at the Doheny Eye Centers between 2010 and 2015. The fovea-centered 512 × 128 cubes (6 × 6 mm) acquired with a SD-OCT tomography system (Cirrus HD-OCT; Carl Zeiss Meditec, Dublin, CA, USA) were selected and evaluated by two certified readers in order to ensure their high quality.

Eligible patients had intermediate AMD (determined by clinical examination and confirmed by OCT) at least in one eye and no evidence of any other pathology involving the macula. Eyes with nonvisually significant vitreoretinal interface disease, such as a subtle epiretinal membrane only visible by OCT, were not excluded. All eligible patients needed to have follow-up for at least 12 months, including OCT imaging. When both eyes were eligible, the right eye was chosen for analysis.

Data collection was approved by the institutional review board (IRB) of the University of California – Los Angeles (UCLA). The study was performed in accordance with the Health Insurance Portability and Accountability Act and adhered to the principles of the Declaration of Helsinki. A waiver of informed consent was granted by the IRB for this retrospective analysis.

OCT Grading

All study eyes were assessed at baseline and follow-up for DV, EZ normalized reflectivity, and HRF presence and quantity. The DV within 3- and 5-mm circles centered on the fovea were automatically generated by the instrument software (Cirrus Advanced RPE analysis software, v. 8.0; Carl Zeiss Meditec).[9,10]

En face EZ normalized reflectivity was measured using a previously reported procedure.[11] Briefly, the en face image of the EZ (slab 21 μm thick with inner boundary located 45 μm above the RPE reference) was exported, and the mean brightness was calculated as the mean gray level in the circle region of interest (cROI) centered on the fovea (2-mm radius); this value was then normalized using the reflectivity of the vitreous (in the cROI) and retinal nerve fiber layer (RNFL) (in a region of interest on the nasal sector [nROI; area of 1.11 mm^2]) as dark and bright reference standards, respectively, using the following formula:

$$\text{EZ normalized reflectivity} = \frac{\text{EZ mean reflectivity [cROI]} - \text{Vitreous mean reflectivity [cROI]}}{\text{RNFL mean reflectivity [nROI]}}. \quad (1)$$

As the repeatability of the DV algorithm and EZ normalized reflectivity calculation have been reported previously,[11,15] they were not reassessed in the present study.

Using conventional reading center practices, HRF was deemed present if the grader had >90% confidence that it was present in at least one B-scan. For HRF quantification in eyes that had HRF present, five consecutive en face slabs from the inner limiting membrane to the inner surface of RPE, each representing 20% of the retinal thickness, were extracted and imported into software (ImageJ version 1.50; National Institutes of Health, Bethesda, MD; available at http://rsb.info.nih.gov/ij/index.html).[16] To isolate the areas of HRF, a threshold determined by the standard deviation of the en face image of the midretina slab from a normal database was applied to each retinal slab:

$$HRF = \sum_{i,j=1}^{i,j=672} I(i,j) > I_{\text{mean}} + 2\text{SD}, \quad (2)$$

where I_{mean} indicates the mean value of the entire image; i,j represents the row and column indices of the image with a maximum value of 672 × 672 in the nominal 6 × 6-mm images; and SD is the standard deviation of the midretina en face slab obtained from normal data (20 eyes of 20 healthy subjects). This threshold, applied to normal eyes, allows an almost complete disappearance of the structure with a brightness below that of the RPE (Fig. 1).

The use of five consecutive thin slabs instead of a single thick slab spanning from the RNFL to the EZ was utilized because thinner slabs are better suited for depicting coplanar structures with less risk of superimposition of axially aligned structures compared with thicker sections.[17] After the binarization, the five slabs were manually refined and confirmed by inspection of corresponding B-scans. The manual adjustments of the en face slabs were important to ensure that hyperreflective artifacts such as large vessel walls or portions of the RNFL did not confound the HRF measurement (Fig. 2).

After creating a virtual stack with the five slabs, images were combined using the software function "Z-project," with the selection of "Max Intensity" as the projection type. The resultant image was binarized using the Otsu thresholding method, and the HRF were measured using the ImageJ function "Analyze Particles." We set the plugin to measure all the particles in the binarized image, regardless of size and circularity (parameters of inclusion were size: 0 to infinity; circularity: 0–1). The output gives information about the count and characteristics (total area, average size, and percentage of total area) of the HRF. HRF were measured in the whole image (HRF_{TOT}) and in the central 3-mm (HRF_{3mm}) and 5-mm (HRF_{5mm}) areas (Fig. 3). Interoperator repeatability of HRF measurements was tested in 40 eyes randomly selected among patients with HRF present at baseline.

In the follow-up visits, presence of atrophy or possible CNV were considered to be evidence of AMD progression. Atrophy

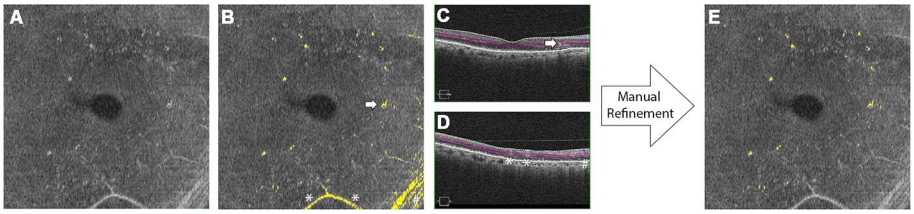

Figure 2. Manual refinement of en face slab (**A**) before quantitative analysis. After the thresholding (**B**), any signals from vessels (*) or nerve fiber layer (NFL) (#) were removed, retaining only signals derived from HRF (*white arrows*), as verified by inspection of corresponding B-scans (**C**, **D**). The resulting en face image where only signals from HRF are highlighted (*yellow pixels*) (**E**).

(complete RPE and outer retinal atrophy or cRORA) was defined using the Classification of Atrophy Meeting (CAM) criteria[18] as hypertransmission of OCT signal into the choroid (at least 250 μm in diameter) with an overlying RPE defect and thinning of the outer retina. A pigment epithelial detachment was considered suspicious for CNV based on its shape (irregular elevation), heterogeneous internal reflectivity, and/or presence of exudation (intraretinal, subretinal, sub-RPE fluid).[19] In this analysis, all cases considered to have CNV also had evidence of exudation. OCT angiography was not obtained.

All OCT analyses were performed by two trained, certified Doheny Image Reading Center OCT graders (MN, WF). The first grader reviewed all cases; the second grader independently reviewed a randomly selected sample of 40 study eyes to assess the intergrader repeatability. Any case of disagreement was assessed by open adjudication. If no consensus was reached, the grading protocol dictated that a final decision was to be made by the emeritus medical director of the reading center (SRS).

Statistical Analysis

All analyses were performed using statistical software (SPSS Statistics v 21.0; IBM Corp., New York, NY, USA). Interoperator repeatability was assessed calculating the intraclass correlation

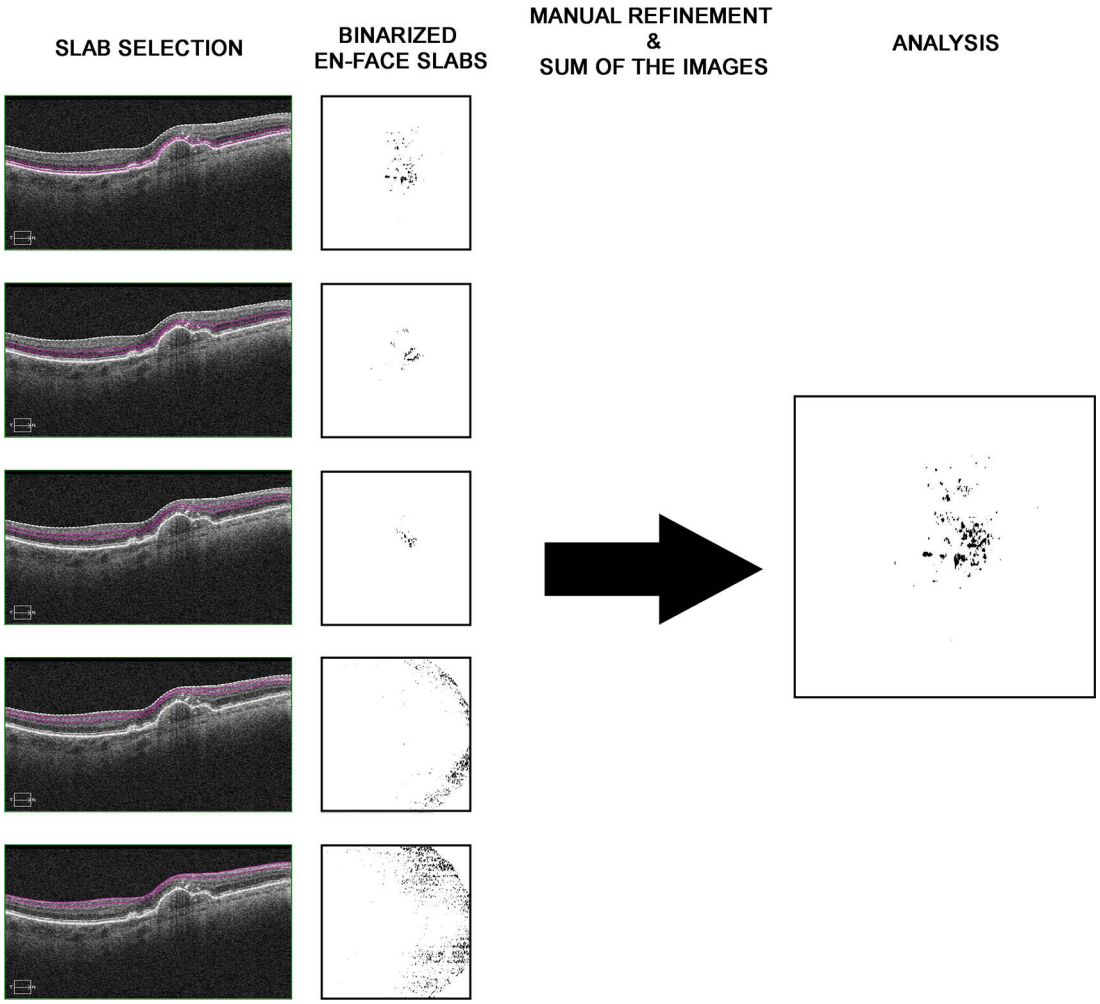

Figure 3. Five consecutive en face slabs from the inner limiting membrane to the inner surface of the RPE, each representing 20% of the retinal thickness, were analyzed after applying a threshold (*left*); after a manual refinement, images were summed and HRF areas were analyzed (*right*).

Investigative Ophthalmology & Visual Science

Table 1. Pairwise Longitudinal Comparison of the Mean Intraretinal HRF Areas, DV, and EZ Normalized Reflectivity per Study Eye From Baseline to 1 Year of Follow-up

	Baseline, Mean ± SD	1 Year, Mean ± SD	*P* Value
HRF_{3mm}, mm^2	0.0194 ± 0.0476	0.0238 ± 0.0354	0.017
HRF_{5mm}, mm^2	0.0259 ± 0.0827	0.0356 ± 0.0723	0.013
HRF_{TOT}, mm^2	0.0280 ± 0.0961	0.0391 ± 0.0798	0.002
DV 3-mm, mm^3	0.6 ± 0.85	0.58 ± 0.79	0.64
DV 5-mm, mm^3	0.79 ± 1.03	0.79 ± 0.95	0.95
EZ reflectivity	0.61 ± 0.11	0.58 ± 0.13	0.01

P values were determined by the Wilcoxon signed ranked test. SD, standard deviation.

coefficients (ICC). Comparison between groups of patients was made using a Mann-Whitney test. The Wilcoxon signed ranked test was used to assess the difference in the HRF areas; DV and EZ normalized reflectivity between baseline and 1 year of follow-up.

The correlation between all HRF measurements and progression to late AMD at 1 year was analyzed using Spearman's ρ test.

The same method was used to correlate HRF_{3mm} with DV within a 3-mm circle and with EZ normalized reflectivity, respectively, and to correlate HRF_{5mm} with DV within a 5-mm circle at both baseline and follow-up. Comparisons between significant correlations were made with Fisher's r to z transformation and then by comparing the z scores for statistical significance by determining the observed z test statistic.

P values less than 0.05 were considered statistically significant.

Results

Baseline Characteristics

One hundred fourteen eyes of 114 patients (48 males) with intermediate AMD met eligibility criteria for the study. Mean age was 77.54 ± 8.54 (range, 68–87). At baseline, mean DV was 0.6 ± 0.85 mm^3 within the 3-mm circle and 0.79 ± 1.03 mm^3 within the 5-mm circle, while EZ normalized reflectivity was 0.61 ± 0.11. HRF were present in 58 eyes (50.8%) and mean HRF area was 0.0194 ± 0.0475 mm^2 (median, 0; range, 0–0.315), 0.0259 ± 0.0826 mm^2 (median, 0.002; range, 0–0.792), and 0.0280 ± 0.096 mm^2 (median, 0.0035; range, 0–0.952) for HRF_{3mm}, HRF_{5mm}, and HRF_{TOT}, respectively. The cohort was further divided into two subgroups according to the presence of HRF. Patients with HRF had significantly higher values of DV in both 3- and 5-mm circle areas (0.84 ± 0.88 and 1.09 ± 1.09 mm^3, respectively) compared to subjects without HRF at baseline (0.36 ± 0.75 and 0.49 ± 0.87 mm^3, respectively), with $P < 0.001$ for both regions. In contrast, there was no difference between the two groups for EZ normalized reflectivity: 0.59 ± 0.11 in the presence of HRF and 0.63 ± 0.11 in the absence of HRF ($P = 0.15$).

1-Year Characteristics

At 1 year, mean DV was 0.58 ± 0.79 mm^3 within the 3-mm circle and 0.79 ± 0.95 mm^3 within the 5-mm circle. No significant difference was found for DV values between baseline and 1 year. EZ normalized reflectivity was 0.58 ± 0.13, which was significantly reduced from baseline value ($P = 0.01$).

HRF were now present in 67 study eyes (58.7%), and the mean HRF area was 0.0238 ± 0.0354 mm^2 (median, 0; range, 0–0.514), 0.0356 ± 0.0723 mm^2 (median, 0.003; range, 0–0.794), and 0.0391 ± 0.0798 mm^2 (median, 0.004; range, 0–0.874) for HRF_{3mm}, HRF_{5mm}, and HRF_{TOT}, respectively. All HRF area values at 1 year had increased significantly from baseline values ($P = 0.017$ for HRF_{3mm}, $P = 0.013$ for HRF_{5mm}, and $P = 0.002$ for HRF_{TOT}). All HRF, DV, and EZ reflectivity results are summarized in Table 1.

Correlations

HRF_{3mm} showed a significant positive correlation with DV in the 3-mm circle both at baseline ($R = 0.342$, $P < 0.001$) and after 1 year ($R = 0.378$, $P < 0.001$). There was a negative correlation between EZ normalized reflectivity and HRF_{3mm} that was significant at both visits ($R = -0.364$, $P < 0.001$ at baseline and $R = -0.312$, $P = 0.004$ at 1 year). HRF_{5mm} showed a significant correlation with DV in the 5-mm circle ($R = 0.354$, $P < 0.001$ at baseline and $R = 0.341$, $P < 0.001$ after 1 year). No significant differences were found for each correlation between the two visits (Table 2).

Among the cohort, 68 eyes did not progress to late AMD after 1 year of follow-up (group A), while nine eyes (7.9%) and 37 eyes (32.4%) developed CNV (group B) and cRORA (group C), respectively, resulting in the total number of 46 eyes (40.3%) that progressed to late AMD (Fig. 4).

HRF areas at baseline for each group are reported in Table 3.

Group C was significantly different from group A ($P < 0.001$ for all HRF areas) and group B ($P = 0.027$, $P = 0.017$, and $P = 0.017$ for HRF_{3mm}, HRF_{5mm}, and HRF_{TOT}, respectively), while

Table 2. Spearman's ρ Correlation Between HRF Areas and EZ Reflectivity and DV in 3-mm and 5-mm Circle Areas

	Baseline		1 Year		
	HRF_{3mm}	HRF_{5mm}	HRF_{3mm}	HRF_{5mm}	*P* Values
DV 3-mm	$R = 0.342$ ($P < 0.001$)	–	$R = 0.378$ ($P < 0.001$)	–	0.576
DV 5-mm	–	$R = 0.354$ ($P < 0.001$)	–	$R = 0.341$ ($P < 0.001$)	0.523
EZ reflectivity	$R = -0.364$ ($P < 0.001$)	–	$R = -0.312$ ($P = 0.004$)	–	0.566

Progression rate to late-stage AMD

R, Spearman's correlation coefficient. *P* values in the third column were determined after Fisher's r to z transformation, comparing the z scores for statistical significance.

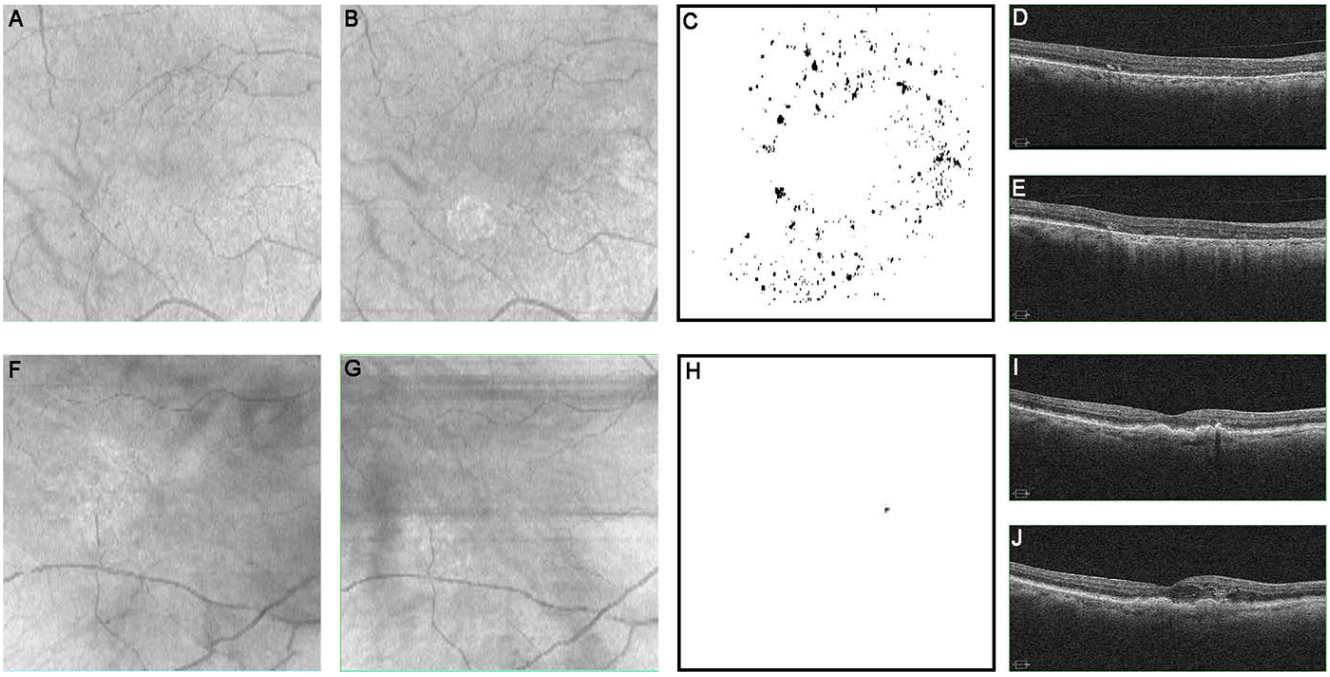

FIGURE 4. (**A**, **B**) Baseline and 1-year OCT fundus photos of a subject who developed to complete RPE and photoreceptor atrophy (cRORA). (**C**) The en face map of the intraretinal HRF as obtained with the method described in the text. (**D**, **E**) The corresponding B-scans passing through the area of cRORA at baseline and after 1 year. (**F**, **G**) The baseline and 1-year OCT fundus photos of a subject who developed CNV. (**H**) The en face map of the HRF. (**I**, **J**) The macular B-scans passing through the area of CNV at baseline and after 1 year.

no significant differences were found between HRF areas in group A versus group C ($P = 0.06$, $P = 0.206$, and $P = 0.253$ for HRF_{3mm}, HRF_{5mm}, and HRF_{TOT}, respectively) (see Fig. 5).

Presence of HRF showed a significant correlation with progression to either cRORA or CNV ($R = 0.454$, $P < 0.001$) or cRORA alone ($R = 0.472$, $P < 0.001$). No correlation was found with CNV development after 1 year ($R = 0.023$, $P = 0.8$). Spearman coefficient values for progression to late AMD were $R = 0.667$ ($P < 0.001$) for HRF_{3mm}, $R = 0.632$ ($P < 0.001$) for HRF_{5mm}, and $R = 0.612$ ($P < 0.001$) for HRF_{TOT}.

Correlations remained significant when considering progression to atrophy alone ($R = 0.692$ ($P < 0.001$), $R = 0.674$ ($P < 0.001$), and $R = 0.657$ ($P < 0.001$) for HRF_{3mm}, HRF_{5mm}, and HRF_{TOT}, respectively), but not for progression to CNV alone ($R = 0.611$ [$P = 0.908$], –0.021 [$P = 0.824$], and –0.027 [$P = 0.777$]). Correlation between HRF and progression to late AMD are shown in Table 4 and Figure 6.

Comparisons between correlations revealed a significant difference between all HRF area measurements and a simple qualitative assessment (i.e., HRF present versus absent) for both progression to late AMD ($P < 0.001$) and to atrophy alone ($P < 0.001$).

Receiver Operating Curve Analysis

Nonparametric receiver operating characteristic (ROC) curves were generated for HRF areas and development of late AMD and cRORA (Fig. 5). Prognostic accuracy of these parameters was determined by calculating the area under the curve (AUC) for each ROC curve.

With respect to progression to late AMD, ROC AUC values (standard error; 95% confidence interval [CI]) were 0.86 (0.04; 0.78–0.93), 0.85 (0.04; 0.77–0.93), and 0.84 (0.04; 0.76–0.92) for HRF_{3mm}, HRF_{5mm}, and HRF_{TOT}, respectively.

With respect to progression to cRORA, ROC AUC values were 0.89 (0.04; 0.81–0.96), 0.89 (0.03; 0.82–0.96), and 0.88 (0.04; 0.81–0.95) for HRF_{3mm}, HRF_{5mm}, and HRF_{TOT}, respectively. These values indicated good prognostic accuracy for all HRF areas to predict the progression to late AMD and in particular to cRORA. Sensitivity and specificity plots as a function of HRF area threshold points were generated (Fig. 5).

Intergrader and Interoperator Repeatability

The unweighted κ value for intergrader repeatability was 0.87 (35/40) for HRF presence and 0.72 (29/40) for late AMD progression. In all the cases with discrepancy between graders, consensus could be achieved following open adjudication and discussion between the two graders, without need for reading center medical director review. Good agreement was also observed for quantitative HRF assessment for all three regions considered: ICC = 0.904 (95% CI: 0.888–0.937) for HRF_{3mm}; ICC = 0.888 (95% CI: 0.851–0.925) for HRF_{5mm}, and ICC = 0.878 (95% CI: 0.855–0.937) for HRF_{TOT}.

TABLE 3. Baseline Mean Values of Intraretinal HRF Areas in All the AMD Cohort Divided by Outcome of Progression: No Progression, Progression to CNV, Progression to Complete RPE, and Photoreceptor Atrophy (cRORA)

	HRF_{3mm}, mm^2	HRF_{5mm}, mm^2	HRF_{TOT}, mm^2
No progression, $n = 68$	0.002 ± 0.005	0.003 ± 0.007	0.004 ± 0.008
Progression to CNV, $n = 9$	0.021 ± 0.04	0.021 ± 0.04	0.022 ± 0.041
Progression to cRORA, $n = 37$	0.051 ± 0.71	0.068 ± 0.134	0.073 ± 0.16

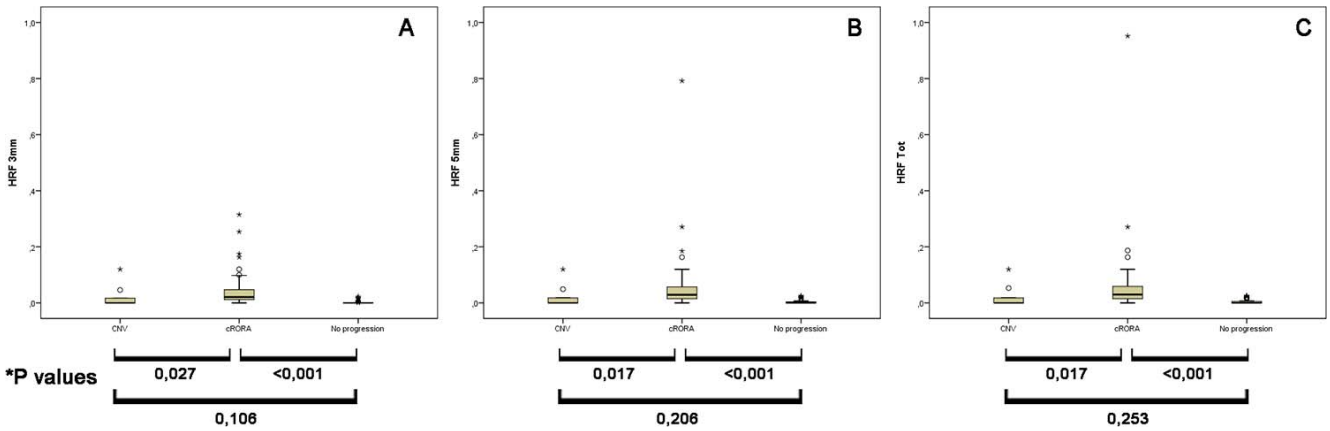

Figure 5. Box plots of (**A**) HRF_{3mm}, (**B**) HRF_{5mm}, and (**C**) HRF_{TOT} at baseline for patients with intermediate AMD with no progression, progression to CNV, or progression to complete RPE and photoreceptor atrophy (cRORA) after 1 year of follow-up. *P* values derive from a Mann-Whitney test between each group, with $P < 0.05$ being statistically significant.

Discussion

The main objective of this study was to determine whether quantitative measurements of areas of HRF could improve the prediction of progression to late AMD compared to qualitative assessments. Several in vivo OCT studies have suggested that HRF in intermediate AMD eyes may represent the migration of activated RPE cells into the inner retinal layers.[5,8,20,21] This hypothesis was supported by some laboratory studies that demonstrated the potential ability of RPE cells to migrate when induced by cytokines and other inflammatory mediators in response to oxidative damage and complement activation.[22,23]

Previous studies[7,24] showed that HRF in AMD were associated or colocalized with the drusen apex and showed an increased association with RPE atrophy at baseline,[24] or if atrophy was not already present, with an increased risk of developing atrophy at that location.[7] Christenbury et al.[8] suggested that the association between HRF and drusen becomes more significant over time with an increasing number of HRF associated with increasing drusen and atrophy. These findings would suggest a potential interest in quantifying the HRF in order to improve the predictability of the disease progression.

The method described in the present study allows the measurement of the HRF in the 6×6-mm OCT macular cube in a semiautomated fashion. Good repeatability was achieved using this approach despite the need for manual refinement and confirmation of proper slab positioning, particularly for the more superficial slabs where large retinal vessels could interfere with assessment of HRF. Such refinements to eliminate these superficial vessels are generally not necessary in the central part of the image and likely account for the higher repeatability for the HRF_{3mm} compared with the other measurements. Moreover, it should be noted that the inter B-scan distance was 46.9 µm, and thus very small HRF could still be missed despite the use of our en face method.

It is worth mentioning that the quantification of intraretinal HRF may be useful not only for AMD but also for other diseases in which HRF are present and can have prognostic value. For example, in central serous chorioretinopathy, although their precise nature is unclear, it has been hypothesized that HRF may be extravasated lipoproteins, activated microglia with phagocytized photoreceptor, or possibly intraretinally migrated RPE.[25] Nevertheless, their presence and number have been associated with the recurrence of the disease and its visual outcome.[26,27]

In diabetic retinopathy, HRF could be a sign of lipid and/or protein extravasation[28] or may represent activated microglial cells.[29] In both cases their quantification may be useful to monitor the progression of the retinopathy and its response to treatmanent.[30]

The semiautomated method for HRF quantification developed in this study may be helpful for systematic analysis of this features in the setting of clinical trials and clinical research. In our study, we demonstrated a significant correlation between HRF quantity and DV, both at baseline and after 1 year, with no significant difference between the two visits. It is of interest that while there was a significant increase in HRF after 1 year, along with the appearance of RPE atrophy, no difference was found in DV. This may be because new drusen appeared as others collapsed and evolved into atrophy. This may also suggest that during a particular drusen's life cycle, several HRF could migrate sequentially at different times until atrophy eventually developed at that location. Lei et al.[4] previously noted that the development of atrophy in the setting of HRF was unsurprising, since migration of the RPE into the retina may leave gaps in the normal RPE monolayer. A closer localized follow-up of these lesions evaluating the quantity of HRF overlying specific drusen may further clarify this point. Another potential explanation that may explain the independent increase in HRF despite stable DV is the presence of SDD. SDD have also been associated with HRF,[4] and since they are not detected by the DV volume algorithm, they could have contributed to the HRF increase over time.

Table 4. Spearman's ρ Correlation Between HRF Areas and Progression to Late AMD (Atrophy or CNV)

	HRF_{3mm}	HRF_{5mm}	HRF_{TOT}	HRF Yes/No
Progression to late AMD	$R = 0.667$ ($P < 0.001$)	$R = 0.632$ ($P < 0.001$)	$R = 0.612$ ($P < 0.001$)	$R = 0.454$ ($P < 0.001$)
Progression to CNV	$R = 0.011$ ($P = 0.908$)	$R = -0.021$ ($P = 0.824$)	$R = -0.027$ ($P = 0.777$)	$R = 0.023$ ($P = 0.8$)
Progression to atrophy	$R = 0.692$ ($P < 0.001$)	$R = 0.674$ ($P < 0.001$)	$R = 0.657$ ($P < 0.001$)	$R = 0.445$ ($P < 0.001$)

R, Spearman's correlation coefficient; *P*, two-tailed *P* value.

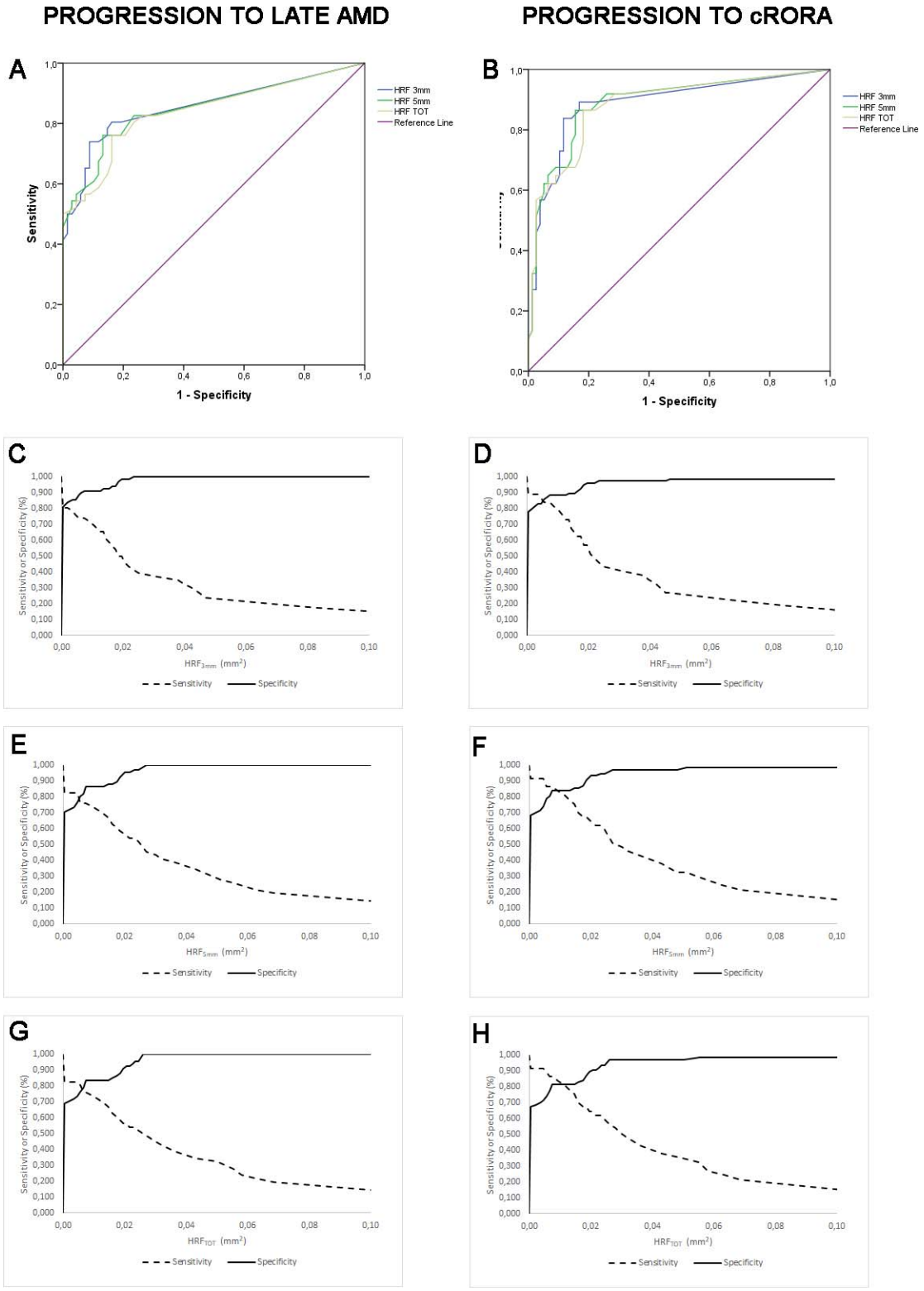

Figure 6. ROC curves for intraretinal HRF area for prediction of late AMD (**A**) or complete RPE and photoreceptor atrophy (cRORA) (**B**) progression after 1 year of follow-up. An AUC of 0.5, corresponding to the diagonal line in each ROC plot, indicates diagnostic accuracy no better than chance, while greater values indicate better diagnostic performance, with a value of 1.0 being perfect. Sensitivity and specificity plots as a function of HRF_{3mm} (**C**, **D**), HRF_{5mm} (**E**, **F**), and HRF_{TOT} (**G**, **H**). The intersection of sensitivity and specificity curves for each parameter is (**C**) 0.0005 mm^2, (**D**) 0.005 mm^2, (**E**) 0.005 mm^2, (**F**) 0.009 mm^2, (**G**) 0.007 mm^2, (**H**) 0.01 mm^2.

Since it has been demonstrated that HRF are associated with photoreceptor thinning,[31] we anticipated that there would be a correlation between HRF and EZ normalized reflectivity. EZ reflectivity values found in our intermediate AMD patients at baseline are comparable to values found previously by Borrelli et al.[11] (0.61 ± 0.09). In our cohort, this value significantly decreased over time, possibly indicating a progression in photoreceptor damage.

Presence of a significant correlation between HRF and EZ reflectivity seems to be consistent with the hypothesis that the more intraretinal HRF are present, the more advanced is the damage. Shadows or signal attenuation produced by HRF at the level of photoreceptors on en face images may have influenced the EZ reflectivity and may be responsible for the observed correlation. On the other hand, the absence of a significant difference in EZ reflectivity between patients with or without HRF would seem to at least partially exclude this possibility.

Lei et al.[4] demonstrated that the presence of HRF is the strongest individual predictor for AMD progression compared with DV $\geq$ 0.03 mm^3 in the central 3-mm area, hyporeflective foci within a drusenoid lesion, and SDD. In our study, measuring HRF quantity instead of simply evaluating its presence seemed to increase the strength of the correlation with progression to late AMD with an R value as high as 0.667 for HRF_{3mm}. A similar significant correlation was observed for progression to atrophy alone at 1 year. We found no significant correlation between HRF quantity and rate of progression to CNV after 1 year of follow-up. This observation would seem to be contrary to our previous publications showing that HRF commonly precede the development of type 3 neovascularization.[4,32] Our present study may have been underpowered, as the event rate for CNV development was low. Further investigation with a large sample and a longer prospective analysis may help to clarify this point. Indeed, the correlations and predictive power of HRF for both cRORA and CNV may have been enhanced with longer follow-up and the development of more events over time. On the other hand, the 1-year progression rate is of value as it may be most relevant to the development of future clinical trials that may be aimed at preventing the development of late AMD.

Our study has several limitations that should be considered when assessing our findings. First, since the cohort was collected retrospectively, the study is subject to selection bias. Second, it may not be reasonable to presume that all HRF are evidence of pigment migration (either RPE cells and/or free melanosome and/or glial cells that have captured released pigment). In the context of eyes that developed CNV, it is possible that some HRF may have been features of exudation. Third, our HRF quantification method is not yet fully automated and does require some manual refinement to exclude large retinal blood vessels. Despite this, we observed a high-level of intergrader repeatability. However, for this to be a clinically useful tool, a fully automated solution will be necessary. Fourth, the lack of axial length data for each eye might have affected the measurements of the HRF since it was not possible to scale each image correctly. However, we believe that it is unlikely that the strong correlations observed in this study could be attributed only to an effect of the axial length.

Our study also has several strengths, including the use of the same OCT device and scanning protocol for all subjects and the use of certified reading center graders for all assessments.

In summary, the quantification of macular HRF in patients with intermediate AMD correlates with photoreceptor damage and the 1-year risk of AMD progression, in particular with cRORA/GA. The amount of macular HRF using en face OCT images may have a potential clinical use in evaluating patients' prognosis and selecting high-risk patients for enrollment in clinical trials.

Acknowledgments

Disclosure: **M. Nassisi**, None; **W. Fan**, None; **Y. Shi**, None; **J. Lei**, None; **E. Borrelli**, None; **M. Ip**, Thrombogenics (C), Omeros (C), Boehringer Ingelheim (C), Genentech (C), Quark (C), Astellas Institute for Regenerative Medicine (C), Allergan (C); **S.R. Sadda**, Allergan (C, F), Carl Zeiss Meditec (C, F), CenterVue (C), Genentech (C, F), Heidelberg Engineering (C), Iconic (C), NightstarX (C), Novartis (C), Optos (C, F), Thrombogenics (C), Topcon (C)

References

1. Bressler NM, Bressler SB, Congdon NG, et al. Potential public health impact of Age-Related Eye Disease Study results: AREDS report no. 11. *Arch Ophthalmol*. 2003;121:1621–1624.
2. Age-Related Eye Disease Study Research Group. A randomized, placebo-controlled, clinical trial of high-dose supplementation with vitamins C and E, beta carotene, and zinc for age-related macular degeneration and vision loss: AREDS report no. 8. *Arch Ophthalmol*. 2001;119:1417–1436.
3. Jack LS, Sadiq MA, Do DV, Nguyen QD. Emixustat and lampalizumab: potential therapeutic options for geographic atrophy. *Dev Ophthalmol*. 2016;55:302–309.
4. Lei J, Balasubramanian S, Abdelfattah NS, Nittala MG, Sadda SR. Proposal of a simple optical coherence tomography-based scoring system for progression of age-related macular degeneration. *Graefes Arch Clin Exp Ophthalmol*. 2017;255:1551–1558.
5. Ho J, Witkin AJ, Liu J, et al. Documentation of intraretinal retinal pigment epithelium migration via high-speed ultrahigh-resolution optical coherence tomography. *Ophthalmology*. 2011;118:687–693.
6. Folgar FA, Chow JH, Farsiu S, et al. Spatial correlation between hyperpigmentary changes on color fundus photography and hyperreflective foci on SDOCT in intermediate AMD. *Invest Ophthalmol Vis Sci*. 2012;53:4626–4633.
7. Ouyang Y, Heussen FM, Hariri A, Keane PA, Sadda SR. Optical coherence tomography-based observation of the natural history of drusenoid lesion in eyes with dry age-related macular degeneration. *Ophthalmology*. 2013;120:2656–2665.
8. Christenbury JG, Folgar FA, O'Connell RV, et al. Progression of intermediate age-related macular degeneration with proliferation and inner retinal migration of hyperreflective foci. *Ophthalmology*. 2013;120:1038–1045.
9. Abdelfattah NS, Zhang H, Boyer DS, et al. Drusen volume as a predictor of disease progression in patients with late age-related macular degeneration in the fellow eye. *Invest Ophthalmol Vis Sci*. 2016;57:1839–1846.
10. Yehoshua Z, Wang F, Rosenfeld PJ, Penha FM, Feuer WJ, Gregori G. Natural history of drusen morphology in age-related macular degeneration using spectral domain optical coherence tomography. *Ophthalmology*. 2011;118:2434–2441.
11. Borrelli E, Abdelfattah NS, Uji A, Nittala MG, Boyer DS, Sadda SR. Postreceptor neuronal loss in intermediate age-related macular degeneration. *Am J Ophthalmol*. 2017;181:1–11.
12. Hood DC, Zhang X, Ramachandran R, et al. The inner segment/outer segment border seen on optical coherence tomography is less intense in patients with diminished cone function. *Invest Ophthalmol Vis Sci*. 2011;52:9703–9709.
13. Pappuru RR, Ouyang Y, Nittala MG, et al. Relationship between outer retinal thickness substructures and visual acuity in eyes with dry age-related macular degeneration. *Invest Ophthalmol Vis Sci*. 2011;52:6743–6748.

14. Ferris FL, Wilkinson CP, Bird A, et al. Clinical classification of age-related macular degeneration. *Ophthalmology*. 2013;120:844–851.
15. Nittala MG, Ruiz-Garcia H, Sadda SR. Accuracy and reproducibility of automated drusen segmentation in eyes with non-neovascular age-related macular degeneration. *Invest Ophthalmol Vis Sci*. 2012;53:8319–8324.
16. Schneider CA, Rasband WS, Eliceiri KW. NIH Image to ImageJ: 25 years of image analysis. *Nat Methods*. 2012;9:671–675.
17. Coscas GJ, Lupidi M, Coscas F, Cagini C, Souied EH. Optical coherence tomography angiography versus traditional multimodal imaging in assessing the activity of exudative age-related macular degeneration: a new diagnostic challenge. *Retina*. 2015;35:2219–2228.
18. Sadda SR, Guymer R, Holz FG, et al. Consensus definition for atrophy associated with age-related macular degeneration on OCT: classification of atrophy report 3 [published online ahead of print November 2, 2017]. *Ophthalmology*. https://doi:10.1016/j.ophtha.2017.09.028.
19. Lee SY, Stetson PF, Ruiz-Garcia H, Heussen FM, Sadda SR. Automated characterization of pigment epithelial detachment by optical coherence tomography. *Invest Ophthalmol Vis Sci*. 2012;53:164–170.
20. Pieroni CG, Witkin AJ, Ko TH, et al. Ultrahigh resolution optical coherence tomography in non-exudative age related macular degeneration. *Br J Ophthalmol*. 2006;90:191–197.
21. Fleckenstein M, Charbel Issa P, Helb H-M, et al. High-resolution spectral domain-OCT imaging in geographic atrophy associated with age-related macular degeneration. *Invest Ophthalmol Vis Sci*. 2008;49:4137–4144.
22. Mitsuhiro MRKH, Eguchi S, Yamashita H. Regulation mechanisms of retinal pigment epithelial cell migration by the TGF-beta superfamily. *Acta Ophthalmol Scand*. 2003;81:630–638.
23. Jin M, He S, Wörpel V, Ryan SJ, Hinton DR. Promotion of adhesion and migration of RPE cells to provisional extracellular matrices by TNF-alpha. *Invest Ophthalmol Vis Sci*. 2000;41:4324–4332.
24. Leuschen JN, Schuman SG, Winter KP, et al. Spectral-domain optical coherence tomography characteristics of intermediate age-related macular degeneration. *Ophthalmology*. 2013;120:140–150.
25. Kon Y, Iida T, Maruko I, Saito M. The optical coherence tomography-ophthalmoscope for examination of central serous chorioretinopathy with precipitates. *Retina*. 2008;28:864–869.
26. Lee H, Lee J, Chung H, Kim HC. Baseline spectral domain optical coherence tomographic hyperreflective foci as a predictor of visual outcome and recurrence for central serous chorioretinopathy. *Retina*. 2016;36:1372–1380.
27. Matet A, Daruich A, Zola M, Behar-Cohen F. Risk factors for recurrences of central serous chorioretinopathy. *Retina*. 2018;38:1403–1414.
28. Bolz M, Schmidt-Erfurth U, Deak G, et al. Optical coherence tomographic hyperreflective foci: a morphologic sign of lipid extravasation in diabetic macular edema. *Ophthalmology*. 2009;116:914–920.
29. Vujosevic S, Bini S, Midena G, Berton M, Pilotto E, Midena E. Hyperreflective intraretinal spots in diabetics without and with nonproliferative diabetic retinopathy: an in vivo study using spectral domain OCT. *J Diabetes Res*. 2013;2013:491835.
30. Srinivas S, Nittala MG, Hariri A, et al. Quantification of intraretinal hard exudates in eyes with diabetic retinopathy by optical coherence tomography. *Retina*. 2018;38:231–236.
31. Schuman SG, Koreishi AF, Farsiu S, Jung S, Izatt JA, Toth CA. Photoreceptor layer thinning over drusen in eyes with age-related macular degeneration imaged in vivo with spectral-domain optical coherence tomography. *Ophthalmology*. 2009;116:488–496.e2.
32. Nagiel A, Sarraf D, Sadda SR, et al. Type 3 neovascularization: evolution, association with pigment epithelial detachment, and treatment response as revealed by spectral domain optical coherence tomography. *Retina*. 2015;35:638–647.

Investigative Ophthalmology & Visual Science